International Journal of Heat and Technology
Vol. 42, No. 6, December, 2024, pp. 2008-2018
Journal homepage: http://iieta.org/journals/ijht

Refined Assessment of Thermodynamic Effects of Urban Green Spaces Based on GIS Technology and Optimization of Their Layout Strategy

Shuang Lu*, Lei Kong, Yi Liu, Qian Zhang, Dan Zhang, Mengjing Wang

School of Art and Design, Zhengzhou University of Light Industry, Zhengzhou 450002, China

Corresponding Author Email: 2004009@mail.zzuli.edu.cn

https://doi.org/10.18280/ijht.420618

Received: 17 June 2024
Revised: 22 October 2024
Accepted: 2 November 2024
Available online: 31 December 2024

Keywords:
urban green spaces, thermodynamic effects, GIS technology, heat island effect, spatial analysis, layout optimization

ABSTRACT

As urbanization continues to accelerate, the urban heat island effect has become an increasingly severe environmental issue globally. Urban green spaces, as an important form of green infrastructure, have significant thermodynamic effects that can effectively regulate urban temperatures, alleviate the heat island effect, and improve the urban climate. However, with the expansion of cities and the reduction of green spaces, the thermodynamic effects of these spaces have not been fully utilized, and urban thermal environment issues have become more pronounced. Therefore, researching the thermodynamic effects of urban green spaces and optimizing their layout has become a crucial topic in urban environmental planning and management. Current studies primarily focus on the macroscopic evaluation of thermodynamic effects of urban green spaces through remote sensing data, meteorological monitoring, and other methods. However, these studies often neglect spatially refined analysis and fail to accurately reveal the thermodynamic effects of urban green spaces at different scales and across various types. Additionally, existing methods mainly focus on single-factor impacts, lacking a comprehensive analysis of the relationship between green space thermodynamic effects and factors such as urban morphology and land use. Therefore, a refined assessment method based on GIS technology and a comprehensive analysis of influencing factors are urgently needed to improve the accuracy and applicability of evaluating the thermodynamic effects of urban green spaces. This paper aims to conduct a refined assessment and layout optimization study of urban green space thermodynamic effects based on GIS technology. The research includes two main parts: first, using GIS technology to spatially represent the thermodynamic effects of urban green spaces, with detailed analysis through indicators such as thermodynamic effect footprints, effect capacity, and effect centers; second, combining GIS technology to perform a correlation analysis of the main influencing factors of urban green space thermodynamic effects and propose optimization strategies for green space layout based on effect evaluation. This study will provide a theoretical basis for urban green space planning and optimization and offer data support for mitigating the urban heat island effect and improving urban environmental quality.

1. INTRODUCTION

With the continuous advancement of urbanization, urban heat islands have become an important issue affecting urban climate, ecological environment, and residents' health [1-5]. Urban green spaces, as key elements in regulating urban climate and alleviating the heat island effect, play a crucial role in improving urban environmental quality through their thermodynamic effects. However, with the gradual reduction in the area of urban green spaces and the rapid pace of urbanization, the thermodynamic effects of green spaces have not been fully realized, leading to the deterioration of the urban thermal environment [6-11]. Therefore, how to refine the assessment of the thermodynamic effects of urban green spaces and enhance their role through optimized layout has become a hot topic in urban planning and environmental management.

In this context, research on the assessment of thermodynamic effects of urban green spaces and optimization of their layout based on GIS technology has significant scientific and practical value [11, 12]. First, using GIS technology to spatially represent the thermodynamic effects of urban green spaces can accurately describe the heat regulation effect of different types of green spaces at different scales, providing data support for urban green space planning and management. Second, combining GIS technology to systematically analyze the factors affecting the thermodynamic effects of green spaces helps to reveal the intrinsic relationships between green spaces and various factors such as climate change, urban morphology, and land use, thus providing more precise optimization strategies for alleviating urban heat island effects [13-16]. Therefore, in-

depth research on the thermodynamic effects of urban green spaces based on GIS technology can not only provide a theoretical basis for the scientific planning of urban green infrastructure but also offer decision support for sustainable urban development.

Although some progress has been made in the assessment and optimization of the layout of urban green spaces' thermodynamic effects, there are still significant shortcomings [17-19]. Many existing studies rely on traditional remote sensing data and meteorological data for macroscopic evaluation, neglecting the fine spatial expression of the thermodynamic effects of urban green spaces, leading to significant uncertainty in the evaluation results [20-24]. Furthermore, most existing studies focus on the impact of single factors, lacking comprehensive analysis of the interactions between multiple influencing factors, which limits the application of the research results in the optimization layout of urban green spaces. Therefore, existing assessment methods still need further improvement in terms of precision, comprehensiveness, and practicality.

This paper aims to refine the assessment and optimization of urban green space thermodynamic effects by introducing GIS technology, combined with spatial indicators such as thermodynamic effect footprints, effect capacity, and effect centers. Specifically, the research content of this paper is divided into two parts: the first part is the expression of urban green space thermodynamic effects based on GIS technology, focusing on accurately describing the heat regulation effect of urban green spaces on the thermal environment through spatial data analysis and modeling, the second part is the correlation analysis of factors influencing urban green space thermodynamic effects and its optimization layout based on GIS technology, aiming to propose optimization strategies for urban green space layout by comprehensively considering various influencing factors. This research not only fills the gap in the assessment of urban green space thermodynamic effects but also provides scientific decision support for urban planning and environmental management, with significant theoretical and practical implications for improving urban ecological environment quality.

2. EXPRESSION OF URBAN GREEN SPACE THERMODYNAMIC EFFECTS BASED ON GIS TECHNOLOGY

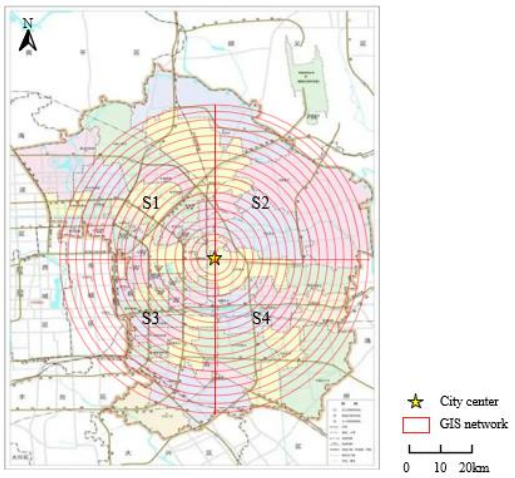

Figure 1. Example of GIS grid establishment

GIS grid technology divides the study area into regular grid units, assigning corresponding thermodynamic data to each grid. These data include surface temperature, humidity, radiative heat flux, and other factors, as well as the distribution, type, and coverage of green spaces. In this study, GIS grid technology will serve as a spatial analysis tool to effectively quantify and visualize the thermodynamic effects of urban green spaces. This technology provides a high-precision spatial analysis method with strong spatiotemporal analysis capabilities, allowing researchers to assess thermodynamic effects both locally and overall at different spatial scales. Figure 1 shows an example of the establishment of GIS grids.

2.1 Calculation of urban green space thermodynamic effect indicators based on GIS grids

To accurately analyze the spatiotemporal distribution characteristics of the thermodynamic effects of urban green spaces, this study selects three spatial indicators: urban green space thermodynamic effect footprint, urban green space thermodynamic effect capacity, and urban green space thermodynamic effect centroid, to describe the significance and spatial distribution of the thermodynamic effects of urban green spaces.

Before quantifying the urban green space thermodynamic effect footprint, thermodynamic effect capacity, and thermodynamic effect centroid, this study first quantifies the intensity of urban green space thermodynamic effects. This indicator refers to the ability of urban green spaces to influence the thermodynamic state of the surrounding environment through their surface temperature regulation effect on a specific time and spatial scale. It reflects the strength of the thermodynamic effects generated in the local climate by urban green spaces through processes such as evapotranspiration, heat absorption, and radiation. The intensity of this effect is closely related to the area, type, and distribution of the green space, as well as factors such as geographical environment, climate conditions, and human activities. The calculation of this indicator is mainly done by grid-processing the urban area to quantify the thermal regulation effect of the green space in each grid unit. Specifically, the study area is first divided into uniform grid units, where the size of each grid H can be flexibly adjusted based on the spatial scale of the study. In each grid, the thermodynamic effect of the green space is quantitatively analyzed by comparing the surface temperature S_H of the grid with the surrounding urban background temperature S_{GR}. The surface temperature S_H represents the actual measured or calculated temperature value within the grid, while the urban background temperature S_{GR} refers to the background temperature of the region where the grid is located, typically obtained by averaging the temperature of non-green areas in the city or using model estimations. The temperature difference between the two reflects the strength of the thermodynamic effect generated by the green space in that region, referred to as the urban green space thermodynamic effect intensity QD_H. The specific calculation formula is as follows:

$$QD_H = S_H - S_{GR} \qquad H = 1, 2...v \tag{1}$$

Assuming the total number of surface temperature values in the background temperature field region is represented by j, the calculation of S_{GR} is as follows:

$$S_{GR} = \sum_{u=1}^{j} S_u / j \quad (2)$$

The urban green space thermodynamic effect footprint refers to the spatial extent affected by the heat exchange between urban green spaces and the surrounding environment over a specific period. This indicator mainly reflects the impact of urban green spaces on regulating the local climate, especially the regulation of thermodynamic characteristics such as temperature and humidity. Through GIS grid technology, the thermodynamic effect footprint can be precisely described through spatial distribution data, reflecting the specific impact range of green spaces on the urban environment. The thermodynamic effect footprint of green spaces is influenced not only by the type and area of the green space but also by the thermodynamic properties of the urban area in which they are located. The calculation principle of this indicator is to identify and quantitatively calculate the green areas with thermodynamic effects through the division of grid units. In the study area, the appropriate grid scale is first determined using a grid encoding method, and the area of each grid is set based on the spatial scale of the study area. Then, for each grid, the urban green space thermodynamic effect intensity is calculated. Specifically, when the thermodynamic effect intensity of green space in the grid is greater than 0, it indicates that the green space within the grid has a significant cooling or heat-relief effect on the environment, and this grid is defined as a "city green space thermodynamic effect footprint area" with a positive effect. After determining the "city green space thermodynamic effect footprint area," further calculations include counting the total number of such areas, summing the grids, and finally obtaining the total thermodynamic effect footprint of urban green spaces within the entire study area. The specific procedure is to count the total number of grids with thermodynamic effect intensities greater than 0 and add up the area values of these grids to obtain the total area of the green space thermodynamic effect footprint. Assuming the footprint of a single grid is represented by DO_H, the total footprint of the study area is represented by DO_{TIL}, and the total number of grids in the study area with a heat island intensity greater than 0 is represented by l, the calculation is as follows:

$$DO_{TIL} = \sum_{H=1}^{l} DO_H \quad (3)$$

The above process is automated by the spatial analysis functions of the GIS system, which efficiently and accurately yields the spatial distribution and total area of the green space thermodynamic effect footprint.

Urban green space thermodynamic effect capacity refers to the total amount of heat that urban green spaces can absorb, store, or release over a specific period. This indicator is typically expressed as the heat exchange per unit area or unit time, reflecting the heat regulation capacity of green spaces on the environment. Different types of green spaces vary in thermodynamic effect capacity. For example, forest green spaces, due to the transpiration of trees and their higher heat capacity, typically have a stronger ability to absorb and store heat, while grasslands or shrubs focus more on regulating the surrounding thermal environment through evaporation and radiative heat dissipation. Using GIS grid technology, researchers can spatially analyze the thermodynamic characteristics of different types of green spaces and accurately measure their heat exchange capacity in specific areas. Unlike traditional surface fitting methods, the calculation of this indicator in this study uses a gridded framework, converting the calculation of the urban green space thermodynamic effect capacity into a calculation of grid volume. In this method, the urban green space thermodynamic effect intensity QD_H of each grid is regarded as the height component of the grid, while the thermodynamic effect footprint DO_H of the green space in the grid represents the horizontal area component. By this simplified spatial representation, errors caused by complex multi-peak surface fitting are avoided, as well as the complex calculations of surfaces with large variations, improving the precision and efficiency of the thermodynamic effect capacity calculation. Specifically, the urban green space thermodynamic effect capacity N_{QD} of each grid can be obtained by multiplying the thermodynamic effect intensity QD_H within the grid by the area of the grid, as follows:

$$N_{QD_H} = DO_H \times QD_H \quad (4)$$

$$N_{QD_{TIL}} = \sum_{u=1}^{l} N_{QD_H} \quad (5)$$

Through the above methods, the total urban green space thermodynamic effect capacity within the research area is obtained by summing the capacities of all grid cells. Using the spatial analysis function of GIS technology, the system calculates and accumulates the urban green space thermodynamic effect capacities of all grid cells, thus obtaining the total thermodynamic effect capacity for the entire area.

Figure 2. Example of the migration of the thermodynamic effect centroid of urban green space

The thermodynamic effect centroid of urban green space refers to the spatial center of the thermodynamic effects of urban green space within a certain range. It is commonly used to represent the concentration trend of the thermodynamic influence of green space on surrounding areas. This indicator helps analyze which regions are most affected by the thermodynamic effects of green space, thereby revealing the spatial distribution characteristics of these effects. The thermodynamic effect centroid can be calculated by weighting the thermodynamic effect values and spatial locations of each

grid cell. This indicator aids researchers in identifying "hotspot" areas of urban green space thermodynamic effects and analyzing how these areas are influenced by green space regulation, further exploring the relationship between green space layout and urban heat island effects. Unlike traditional Gaussian fitting methods, this study calculates the indicator by referring to the calculation method of population centroid. By weighting the temperature of the grid's longitude and latitude, the spatial distribution centroid of urban green space thermodynamic effects is determined. Specifically, the research area is divided into multiple grid cells, with the center point of each grid being considered its spatial location. Then, for each grid, the thermodynamic effect intensity of urban green space is calculated and used as a weight to perform a weighted average of the grid center's longitude and latitude. Through this weighted calculation, the longitude and latitude of the thermodynamic effect centroid for the entire research area are obtained, reflecting the main spatial direction and distribution characteristics of the green space thermodynamic effects. Figure 2 shows an example of the migration of the thermodynamic effect centroid of urban green space based on GIS technology. Additionally, to further improve the calculation of the thermodynamic effect centroid, this paper also introduces the average thermodynamic effect intensity to calculate the height of the thermodynamic effect centroid. Specifically, the average thermodynamic effect intensity for all grids is first calculated, and this average is used as the height component of the thermodynamic effect centroid. Let the longitude, latitude, and height of the heat island centroid be represented by M_S, Y_e, and G_S, respectively, and let the total number of grids in the study area be represented by v. The specific calculation formulas are as follows:

$$M_S = \sum_{u=1}^{v} \left(QD_u * M_u\right) \Big/ \sum_{u=1}^{v} QD_u \tag{6}$$

$$Y_S = \sum_{u=1}^{v} \left(QD_u * Y_u\right) \Big/ u \sum_{i=1}^{v} QD_u \tag{7}$$

$$G_S = \sum_{u=1}^{v} QD_u \tag{8}$$

The transfer contribution rate F of the thermodynamic effect centroid of urban green space can reflect the impact of each region's urban green space thermodynamic effect centroid on the overall migration of the urban green space thermodynamic effect centroid, as expressed by the following formula:

$$F = \left[Z_{f1} * COS\left(Z_{\phi} - Z_{\phi 1}\right)\right] \Big/ Z_f \tag{9}$$

2.2 Expression of the spatial form of urban green space thermodynamic effects

This paper further proposes the expression of the spatial form of urban green space thermodynamic effects based on GIS grid technology. The aim is to visualize the spatial distribution of urban green space thermodynamic effects in three-dimensional space, thereby more precisely describing the regulation effects of urban green space on the thermal environment. This study constructs a grid-based two-dimensional temperature distribution model by combining the thermodynamic effect intensity of urban green space in each grid with the corresponding surface temperature value. These temperature values are then used as height components to form "temperature columns," showing the three-dimensional spatial form of urban green space thermodynamic effects. This method not only retains the spatial distribution characteristics of grid cells but also makes the spatial form of urban green space thermodynamic effects more intuitive and detailed by using the surface temperature value of each grid as the column height, making it easier to identify the spatial differences in thermodynamic effects in different regions.

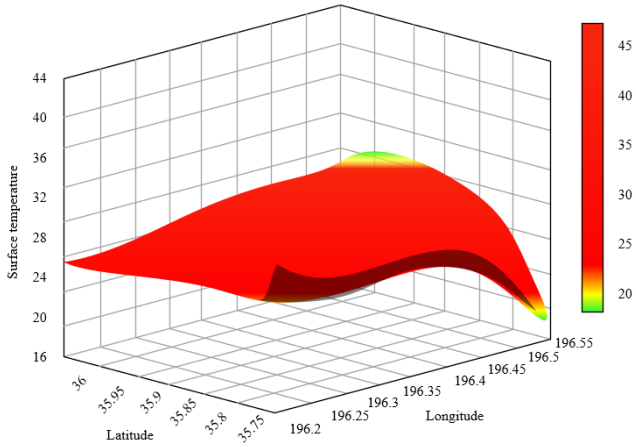

Figure 3. Example of the spatial form expression of urban green space thermodynamic effects

However, the expression of the spatial form of urban green space thermodynamic effects requires balancing modeling accuracy and computational efficiency. Considering the multi-level characteristics of grids, this paper proposes a multi-scale expression method to address the high computational demand caused by high-precision modeling. In this method, the spatial resolution is adjusted by selecting appropriate grid levels based on the characteristics and objectives of the research area. For large areas, a lower grid level is used to improve computational efficiency, while the temperature values of lower-level grids are set to the average temperature of the grids in the upper level to maintain a balance between accuracy and expression efficiency. For local areas with significant thermodynamic effects, a higher grid level is maintained to finely display the spatial form and thermodynamic effect details of these areas. This multi-scale strategy ensures that the overall spatial form expression efficiency is maintained while allowing for more precise analysis of significant urban green space thermodynamic effects, avoiding excessively large computational loads. Figure 3 shows an example of the spatial form expression of urban green space thermodynamic effects.

In the specific visualization of the spatial form of thermodynamic effects, this study implements intuitive spatial distribution presentation by categorizing the thermodynamic effect intensity of urban green space into different levels. Referring to existing quota division methods, this paper classifies the thermodynamic effect intensity of urban green space into five regions: low intensity, second-lowest intensity, medium intensity, second-highest intensity, and high intensity. These classifications are visualized using a color map, allowing clear presentation of regions with different thermodynamic effect intensities. However, when studying regions with high thermodynamic effect intensities, given the wide range of intensities, it is difficult to accurately express the spatial distribution details within high-intensity regions. Therefore, this paper introduces a new "extremely high intensity" level. The introduction of the "extremely high

intensity" level makes it possible to more clearly identify more significant thermodynamic effect regions within the high-intensity areas, providing more precise data support for subsequent temporal and spatial variation analysis and green space thermal regulation strategies.

3. GIS-BASED ANALYSIS OF FACTORS AFFECTING THE THERMODYNAMIC EFFECTS OF URBAN GREEN SPACES AND THEIR OPTIMAL LAYOUT

3.1 Calculation method of influencing factors

The main factors affecting the thermodynamic effects of urban green spaces include land use types and socio-economic factors. To accurately reflect the correlation between these factors and thermodynamic effects, this paper establishes a grid-based correlation model, which creates a one-to-one correspondence between the thermodynamic effects of urban green space and various influencing factors at different scales, thus enabling multi-scale fine calculation. Specifically, the analysis of land use types primarily relies on the normalized difference vegetation index (NDVI) and the normalized difference built-up index (NDBI). These indices, obtained through remote sensing imagery, can be precisely assigned to each grid cell on the GIS platform, enabling the calculation of corresponding thermodynamic effect values for each grid. In this framework, these two indices serve as representative indicators of land use types, and by correlating them with the thermodynamic effect values in each grid, they help identify and quantitatively analyze the contributions of different land use types to the thermodynamic effects of urban green spaces.

Regarding socio-economic factors, since data such as regional GDP and industrial production values cannot be refined to the grid level of the study area, this paper selects population density as the main socio-economic indicator for analysis. Population density can better reflect the intensity of social activities in a region and its potential impact on the thermodynamic effects of urban green spaces. Based on grid technology, population density data is first divided by district, and the total population density for each district is weighted by the spatial relationship between administrative boundaries and grid cells to obtain the precise population density value for each grid. The correlation analysis between this value and the thermodynamic effects of urban green space will reveal the impact of population density on the spatial distribution of these effects, especially in high-density urban areas, where the heat island effect may be more pronounced.

The GIS grid-based correlation model constructed in this paper not only enables the derivation of the relationship between land use types and thermodynamic effects but also analyzes the spatial contributions of socio-economic indicators to the thermodynamic effects of urban green spaces. This multi-factor fine analysis helps urban planners identify areas with the most significant thermodynamic effects and further optimize urban green space layout strategies. Additionally, the model can be adjusted according to different urban planning goals. By modifying the weights of influencing factors, the model can be used to simulate different green space layout scenarios and assess their potential impact on the overall urban thermal environment.

The calculation method for the NDVI primarily relies on the quantitative analysis of vegetation coverage, which reflects the growth condition, health status, and climatic impact of the green space. In this study, the NDVI for the grid center is calculated based on the reflectance difference between the near-infrared band and the red band in remote sensing imagery. First, remote sensing data is used to acquire the reflectance values for the near-infrared and red bands of each grid cell. Specifically, based on image data and predefined grid divisions, the center point location of each grid cell is identified, and then the reflectance values for the near-infrared and red bands at this location are extracted. Let the reflectance of the near-infrared band at the center point of grid H be represented as VUR_H, and the reflectance of the red band at the center point of grid H be represented as E_H. These reflectance values are used to calculate the NDVI using the following formula:

$$NDVI_H = \frac{VUE_H - E_H}{VUE_H + E_H} \tag{10}$$

Since the thermodynamic effects of urban green spaces vary significantly across different regions, higher NDVI values typically indicate higher vegetation coverage and better vegetation health, which suggests that the region may have stronger heat regulation capabilities and can effectively mitigate the heat island effect. In contrast, lower NDVI values indicate sparse or unhealthy vegetation, which may lead to more significant heat island effects in that area. By calculating the NDVI for the center point of each grid, the ecological benefits of urban green space can be accurately reflected, providing support for subsequent fine evaluation of the thermodynamic effects of urban green space. This helps researchers identify areas with lower vegetation coverage and more pronounced thermodynamic effects, allowing for optimized green space layout strategies that maximize the regulation effect on the urban thermal environment. In the layout optimization process, combining NDVI data with the spatial distribution of urban heat island effects can lead to more targeted strategies for increasing and improving green spaces, effectively alleviating the urban heat island effect and improving urban environmental quality.

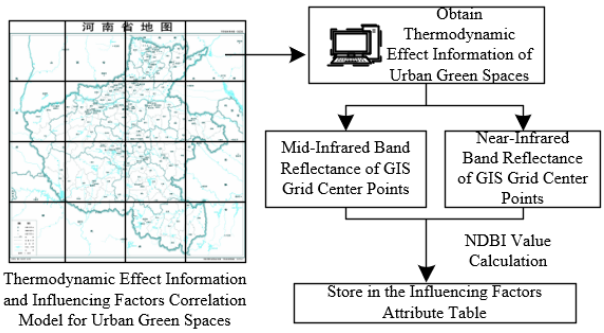

Figure 4. Diagram of the calculation principle of NDBI at the GIS grid center point

NDBI is mainly used to quantify the extent of building coverage in urban areas, with its calculation based on the reflectance difference between the mid-infrared and near-infrared bands. Unlike traditional raster image extraction methods, this paper adopts grid coding technology, calculating the NDBI by locating the reflectance of the mid-infrared and near-infrared bands at the grid center. Figure 4 illustrates the calculation principle of NDBI at the GIS grid center. The specific steps are as follows: First, extract the corresponding mid-infrared and near-infrared reflectance data for each grid

center from remote sensing imagery. Let the NDBI value at the center of grid H be represented by $NDBI_H$, the mid-infrared reflectance at the grid H center by LUE_H, and the near-infrared reflectance at the grid H center by VUE_H. The NDBI can be calculated using the following formula:

$$NDBI_H = \frac{LUE_H - VUE_H}{LUE_H + VUE_H} \tag{11}$$

The NDBI calculated using GIS grid technology will be stored in a grid-based attribute table of the influencing factors of urban green space thermodynamic effects. In this attribute table, the grid code serves as a unique identifier, ensuring a one-to-one correspondence between the NDBI and the thermodynamic effect data of urban green spaces at the grid scale. The establishment of this attribute table not only provides data support for subsequent correlation analysis but also provides researchers with refined spatial data to further evaluate the impact of buildings on urban thermodynamic effects at different scales.

Population density, as a key factor affecting the urban thermal environment, is directly related to the layout of urban green spaces, the extent of heat island effects, and energy consumption. In practice, population density is usually calculated at the administrative district level, that is, the ratio of the resident population to the built-up area in each district. Therefore, this paper first collects the year-end data for the resident population and land area of each district, and calculates the population density for each administrative district. However, since population density data cannot be refined to each grid unit, the average population density of each district needs to be spatially correlated with the land surface temperature of the grid cells within that district. Specifically, the total population density for each district is mapped to the corresponding grid center points based on the location of the grids within the district, ensuring that the population density data is accurately linked to the land surface temperature in space.

To further enhance the comparability of the data and the accuracy of the analysis, this paper standardizes the population density and corresponding land surface temperature of each district using deviation standardization. This step aims to eliminate numerical bias caused by differences in population density across districts and ensures that the analysis is conducted under a unified standard. Specifically, the population density and land surface temperature of each district are standardized so that all data share the same dimension and comparison basis. Let the total population of each district and the land area of each district be represented by PO_{RE} and AR_{RE}, respectively. The standardization formula is typically as follows:

$$OF = \frac{PO_{RE}}{AR_{RE}} \tag{12}$$

3.2 Correlation analysis of influencing factors and the thermodynamic effects of urban green spaces

To gain a deeper understanding of the mechanisms by which various factors influence the urban thermal environment and provide a scientific basis for optimizing the layout of urban green spaces and mitigating the heat island effect, this paper further conducts a correlation analysis of the influencing factors and the thermodynamic effects of urban green spaces. First, based on the NDVI, NDBI, and population density standard values calculated through GIS grid technology, the relationship between different land use types, socio-economic activities, and the thermodynamic effects of urban green spaces is revealed at both the grid and district levels. At the grid scale, the relationship between NDVI and land surface temperature can reveal the dynamic relationship between green space coverage and local temperature variations. Through linear regression analysis of NDVI and land surface temperature, the extent of green space coverage's regulation of the urban thermal environment can be quantitatively assessed, further analyzing the ecological benefits of green spaces and their potential to mitigate the heat island effect. Similarly, the linear fit between NDBI and land surface temperature reveals the impact of urban building density on the local thermal environment. Areas with high NDBI values typically have high building densities, which often lead to the intensification of the heat island effect. Finally, the relationship between the population density standard value and land surface temperature standard value reflects the role of socio-economic activities in the urban thermal environment. High population density areas may exacerbate the heat island effect due to increased energy consumption and land use intensity. Therefore, by conducting linear regression analysis of these three influencing factors, this paper not only reveals the individual effects of each factor but also provides a theoretical basis for subsequent comprehensive impact assessments.

To achieve a refined evaluation of the thermodynamic effects of urban green spaces and optimize their layout, this paper uses the Pearson correlation coefficient to quantitatively analyze the correlation between the influencing factors and land surface temperature. The Pearson correlation coefficient is an important indicator for measuring the strength and direction of the linear relationship between two variables and is widely used in quantitative analysis in environmental science and urban planning. By calculating the Pearson correlation coefficient between NDVI, NDBI, population density standard values, and land surface temperature, the contribution of each factor to the thermal environment can be clearly determined. For example, areas with high NDVI values are typically associated with lower land surface temperatures, reflecting the green space's role in mitigating the heat island effect, areas with high NDBI values are associated with higher land surface temperatures, indicating that densely built-up areas are more prone to forming heat islands, the relationship between population density and land surface temperature reveals the impact of human activities and energy consumption on the urban thermal environment. Let the total sample size used in the analysis be represented by v, and the data values of the two variables by a_u and b_u, with the sample mean values of the two variables denoted as a^- and b^-. The formula for calculating the Pearson correlation coefficient is:

$$e = \frac{\sum_{u=1}^{v}\left(a_u - \bar{a}\right)\left(b_u - \bar{b}\right)}{\sqrt{\sum_{u=1}^{v}\left(a_u - \bar{a}\right)^2 \sum_{u=1}^{v}\left(b_u - \bar{b}\right)^2}} \tag{13}$$

4. EXPERIMENTAL RESULTS AND ANALYSIS

When analyzing the background temperature data of the target city from 2018 to 2023 shown in Table 1, significant seasonal variations can be observed. From the data, it is evident that the background temperature fluctuates noticeably

in the spring. In the spring of 2018, the temperature was 31.25℃, while in the spring of 2020, it dropped to 12.36℃, and in the spring of 2022, it slightly rebounded to 22.58℃, indicating that spring temperatures are highly variable. In contrast, summer temperatures are relatively stable. In the summer of 2018, the temperature was 32.25℃, in the summer of 2020, it was 32.15℃, and in the summer of 2022, it remained at 32.15℃, suggesting that summer temperatures fluctuate less, and the urban heat island effect may be more pronounced in the summer, further impacting the thermal regulation role of urban green spaces. Autumn temperatures show some variation across different years, with the temperature in autumn 2019 being 23.74℃, in autumn 2021 being 25.62℃, and in autumn 2023 dropping to 22.62℃. This reflects that autumn temperature changes may be closely related to the thermodynamic effects of urban green spaces, where the temperature regulation effect of urban green spaces may have been more significant in the autumn. Winter background temperatures are lower, especially in winter 2019 at -0.84℃, winter 2020 at 4.26℃, and winter 2022 at 1.89℃, indicating that the cold winter climate may require enhanced green space planning to alleviate the adverse impacts of low temperatures. Therefore, the variation in background temperature is directly related to the performance of the thermodynamic effects of urban green spaces and affects the ability of different seasons to regulate the thermal environment.

Table 1. Background temperature values of the target city's thermodynamic effect from 2018 to 2023

Date	Background Temperature Value	Date	Background Temperature Value	Date	Background Temperature Value
Spring 2018	31.25℃	Spring 2020	12.36℃	Spring 2022	22.58℃
Summer 2018	32.25℃	Summer 2020	32.15℃	Summer 2022	32.15℃
Autumn 2018	22.36℃	Autumn 2020	18.59℃	Autumn 2022	22.63℃
Winter 2018	4.62℃	Winter 2020	4.26℃	Winter 2022	1.89℃
Spring 2019	24.89℃	Spring 2021	33.26℃	Spring 2023	23.15℃
Summer 2019	33.26℃	Summer 2021	33.74℃	Summer 2023	34.25℃
Autumn 2019	23.74℃	Autumn 2021	25.62℃	Autumn 2023	22.62℃
Winter 2019	-0.84℃	Winter 2021	4.23℃	Winter 2023	5.36℃

Table 2. Thermodynamic effect footprint and growth rate of the target city's core area from 2018 to 2023

Thermodynamic Effect Coefficient / Year	Thermodynamic Effect Footprint (km²)				Thermodynamic Effect Footprint Growth Rate (km²/year)			
	Spring	Summer	Autumn	Winter	Spring	Summer	Autumn	Winter
2018	285.23	645.25	521.23	159.23	-	-	-	-
2019	236.21	658.23	614.23	211.25	-31.25	3.25	88.56	31.256
2020	286.23	612.23	389.23	156.23	32.56	-28.56	-215.23	-31.25
2021	289.21	635.23	612.23	222.32	16.23	17.62	232.25	43.25
2022	432.25	658.23	532.23	189.23	148.26	13.24	-57.261	-22.361
2023	432.59	612.23	568.23	289.23	-5.88	-36.26	25.235	112.03

Table 3. Thermodynamic effect capacity and growth rate of the target city's core area from 2018 to 2023

Thermodynamic Effect Coefficient / Year	Thermodynamic Effect Capacity (km².℃)				Thermodynamic Effect Capacity Growth Rate (km².℃/year)			
	Spring	Summer	Autumn	Winter	Spring	Summer	Autumn	Winter
2018	412.25	4125.23	1124.25	135.28	-	-	-	-
2019	268.23	5216.32	1898.23	129.36	-127.45	1124.23	912.45	-12.36
2020	312.25	3256.17	625.32	114.23	46.25	-2215.26	-1269.52	-32.25
2021	556.34	4658.29	1789.23	215.23	235.28	1586.23	1245.85	124.23
2022	826.59	6325.14	1125.23	223.26	236.21	1648.23	-768.23	-22.32
2023	668.26	2658.23	1248.26	336.89	-142.33	-3625.32	189.66	138.23

From the above analysis, it can be further deduced that for the higher temperatures in spring and summer, the layout and distribution of green spaces should focus on mitigating the heat island effect, increasing the area of green spaces and improving green space coverage to achieve better cooling effects. In autumn and winter, the thermodynamic effects of green spaces can alleviate the discomfort caused by seasonal temperature differences by regulating the rise and fall of temperatures. Therefore, optimizing the layout of green spaces should not only consider the current distribution of green spaces but also integrate geographical features, urban development planning, and climate change to improve the thermodynamic capacity of green spaces while achieving sustainable urban development.

When analyzing the thermodynamic effect footprint and growth rate of the core area of the target city from 2018 to 2023, as shown in Table 2 and Figure 5, the data reveals that the thermodynamic effect footprint fluctuates and changes over time. In the spring of 2018, the thermodynamic effect footprint of the core area was 285.23 km². In subsequent years, it generally showed a growth trend, especially in the spring of 2022 and 2023, where it increased to 432.25 km² and 432.59

km², respectively. The summer and autumn thermodynamic effect footprints showed some volatility. For example, in the summer of 2019, the growth rate of the footprint was 3.25 km²/year, while in the autumn of 2021, the footprint growth reached 232.25 km², but in the autumn of 2022, there was a significant decrease (-57.26 km²). The winter thermodynamic effect footprint changed more steadily, but still exhibited some annual fluctuations. The footprint growth rates for winter from 2019 to 2020 were 31.25 km²/year and -31.25 km²/year, respectively, indicating that seasonal temperature changes had a significant impact on the thermodynamic effect footprint. Overall, from 2018 to 2023, the thermodynamic effect footprint in the core area of the target city showed a general growth trend, but the growth rates varied significantly between seasons, particularly with notable volatility in autumn and winter. This trend may be influenced by the urbanization process, green space coverage, and climate factors.

From the above analysis, particularly in the autumn of 2020 and the winter of 2023, the downward trend in the thermodynamic effect footprint suggests that urban green spaces may not have fully responded to the temperature fluctuations caused by climate change. Therefore, areas with weaker effects can be further identified, and optimization strategies can be proposed based on an assessment of thermodynamic effect capacity and the effect center. During the high-temperature periods in summer, the focus should be on increasing the area of urban green water bodies, using high-efficiency vegetation systems, and increasing permeable materials to reduce the heat island effect. In autumn and winter, measures such as adding temperate vegetation and green roofs can enhance the temperature regulation function of green spaces. In addition, when optimizing layouts, factors such as topography, population density, and transportation networks should be considered to ensure the scientific and sustainable configuration of green spaces.

In Table 3 and Figure 5, the thermodynamic effect capacity and growth rate of the target city's core area from 2018 to 2023 show the dynamic changes of the urban thermal environment, particularly in terms of seasonal fluctuations. From the data, it is evident that the thermodynamic effect capacity in spring is generally low. In 2018, it was 412.25 km².℃, but as the years progressed, it gradually increased. By the spring of 2022, the thermodynamic effect capacity reached 826.59 km².℃, indicating that the thermodynamic effect in spring has gradually strengthened. The thermodynamic effect capacity in summer and autumn showed larger fluctuations in most years. For example, the thermodynamic effect capacity in the summer of 2020 was only 3256.17 km².℃, a significant decrease from 2019, while in the summer of 2021, it rebounded to 4658.29 km².℃, showing that summer climate has a significant impact on thermodynamic effects, which may be related to changes in urban green space coverage, building density, and other factors. The thermodynamic effect capacity in autumn exhibited a significant decrease in 2020 (-1269.52 km².℃), while it rebounded in 2021 to 1789.23 km².℃, but decreased again to 1125.23 km².℃ in 2022, indicating that autumn temperature changes had a clear impact on thermodynamic effects in different years. The thermodynamic effect capacity in winter showed relatively steady changes, with a value of 129.36 km².℃ in winter 2019 and an increase to 138.23 km².℃ by winter 2023. Though the growth rate was slow, it still showed an overall upward trend.

Looking at the growth rates of the thermodynamic effect capacity, the rates in spring and autumn show significant variations, especially in the autumn of 2022 and the spring of 2023, where the growth rate was relatively high. This likely indicates that the thermodynamic effect capacity in these seasons was more significantly affected by climate change and urban green space planning factors.

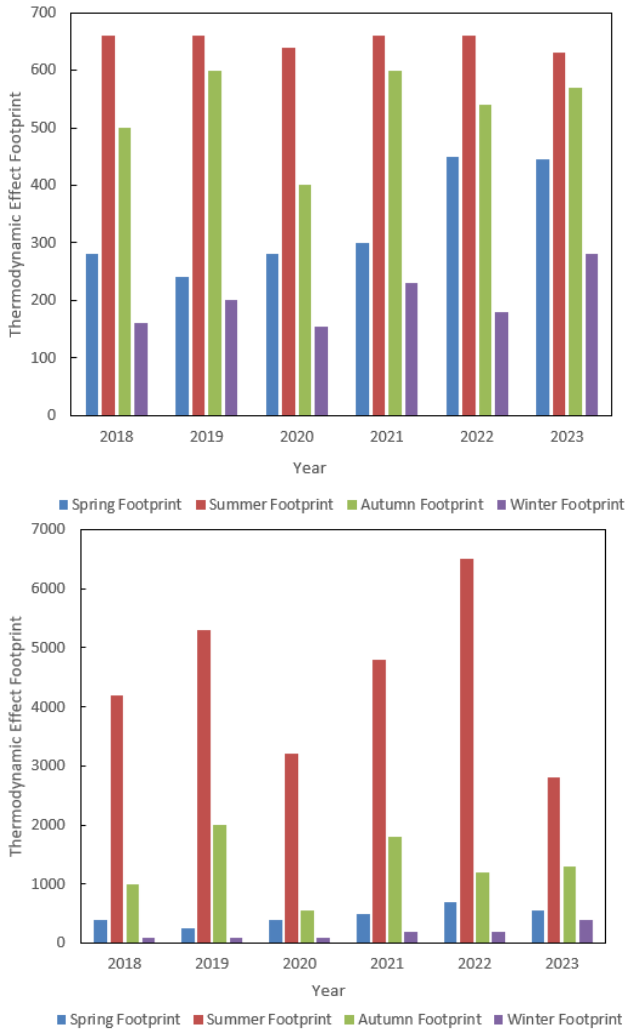

Figure 5. Thermodynamic effect footprint and thermodynamic effect capacity variation with seasons in target cities from 2018 to 2023 (Bar Chart)

Table 4 shows the thermodynamic effect centroid variation in the core area of the target cities from 2018 to 2023, reflecting the spatial transfer trend of thermodynamic effects in the region. From the data, it can be seen that the thermodynamic effect centroid fluctuates in both longitude and latitude, indicating changes in the spatial distribution of thermodynamic effects. For example, in 2019, the thermodynamic effect centroid shifted southwest, with the longitude value decreasing from 123.56 in 2018 to 123.42, and the latitude value increased to 38.562, with a transfer intensity of 4.25. This transfer could be closely related to factors such as urban construction and changes in green space coverage. In 2020, the centroid shifted northeast, with the longitude returning from 123.42 to 123.46 and the latitude dropping to 38.265, with a transfer intensity of -3.26, showing an adjustment in the spatial centroid of the thermodynamic effect. This transfer trend reflects the different distribution characteristics of thermodynamic effects in different urban areas, and over time, the position of thermodynamic effects within the urban space also changes. By 2023, the

thermodynamic effect centroid again shifted southwest, with a transfer intensity of -5.69, indicating that the city's thermodynamic regulation function may have failed to effectively respond to climate change or urbanization, causing the thermodynamic effect centroid to concentrate in certain areas.

Table 4. Thermodynamic effect centroid variation in the core area of the target cities from 2018 to 2023

Date	Longitude Value	Latitude Value	Altitude Value	Transfer Direction	Intensity Change
2018	123.56	38.265	3.56	-	-
2019	123.42	38.562	7.89	Southwest	4.25
2020	123.46	38.265	4.26	Northeast	-3.26
2021	123.28	38.245	7.24	Southwest	2.58
2022	123.37	38.658	9.26	Northeast	2.36
2023	123.35	38.669	3.89	Southwest	-5.69

Combined with the spatial analysis results of thermodynamic effect footprint and capacity, GIS technology can help identify areas with weak thermodynamic effects, providing scientific evidence for optimizing green space configuration. When optimizing the layout, it is recommended to strengthen greening construction in areas where the thermodynamic effect centroid shifts significantly, especially in those with clear transfer directions such as southwest and northeast. By increasing green space areas, improving green space connectivity, and enhancing water and vegetation, the urban heat island effect in specific areas can be effectively mitigated, and the city's thermal environment regulation ability can be improved. Moreover, urban planning should focus on the changes in the thermodynamic effect centroid and adjust the layout of green spaces and infrastructure in a timely manner, considering climate change and urbanization trends, to achieve more efficient thermal environment regulation.

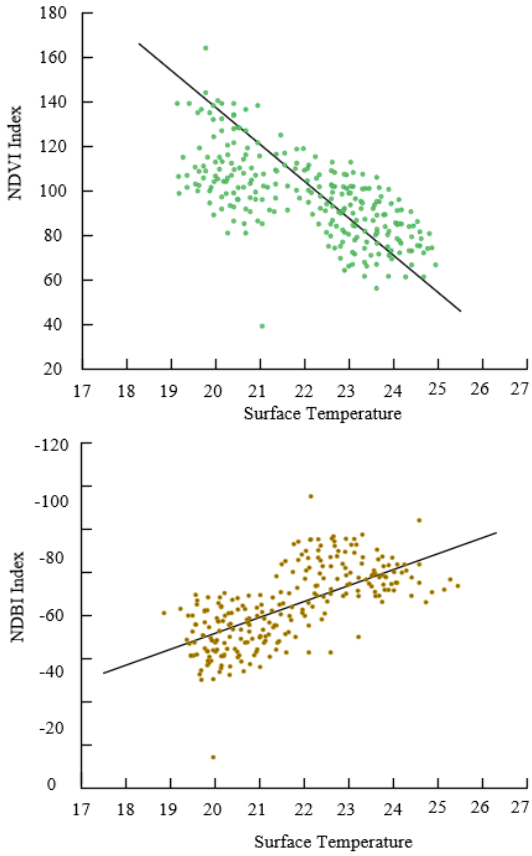

Figure 6. Correlation plot of ground temperature, NDVI, and NDBI in 2023

The experimental results shown in Figure 6 indicate a significant negative correlation between NDVI and the ground temperature, suggesting that increasing urban green space can effectively lower the surface temperature. This finding highlights the important role of green spaces in regulating the urban thermal environment, particularly in addressing the urban heat island effect. At the same time, NDBI is positively correlated with the ground temperature, indicating that an increase in building density leads to higher surface temperatures. These results provide important scientific evidence for urban planning, suggesting that more attention should be paid to the protection and construction of green spaces during urban development.

Based on the above experimental results, this paper proposes optimization strategies for the layout of urban green spaces with thermodynamic effects. First, it is recommended to prioritize increasing green space area, especially in high-temperature areas, to improve the quality of the urban thermal environment. Second, spatial data analysis should be conducted using GIS technology to identify key areas for thermal environment regulation and develop targeted green space layout plans. Additionally, a comprehensive consideration of the relationship between building density and green space distribution is necessary to rationally plan the ratio of buildings to green spaces, achieving harmonious development of the urban ecological environment. These strategies not only help improve the livability of cities but also provide strong support for achieving sustainable development goals.

5. CONCLUSION

This paper, by introducing GIS technology, combines thermodynamic effect footprint, capacity, and centroid spatial indicators to analyze the thermodynamic effects of urban green spaces and provides theoretical support and strategic recommendations for optimizing their layout. In the first part of the study, GS technology was used to refine the thermodynamic effects of urban green spaces, and through spatial data analysis and modeling, the temperature regulation effects of urban green spaces in different seasons and regions were precisely described. Specifically, changes in the thermodynamic effect footprint show that urban green spaces have significantly different temperature regulation effects across seasons, and changes in green space area and layout optimization can effectively mitigate urban heat island effects. The second part analyzes the interactions between green spaces, building density, climate change, and other factors, and proposes green space optimization strategies for different

regions and seasons, aiming to achieve comprehensive optimization of the urban thermal environment.

Comprehensive experimental results show that there is a significant negative correlation between NDVI and ground temperature, meaning that increasing green space area can effectively lower surface temperatures. On the other hand, the positive correlation between NDBI and ground temperature indicates that increasing building density will raise surface temperatures. This finding not only further verifies the important role of urban green spaces in regulating the thermal environment but also provides clear directions for urban green space layout, emphasizing the need to increase green space in high-temperature areas and improve green space structure. However, this study also has certain limitations. First, the study only used surface temperature and vegetation indices as the main analysis indicators, without considering other climatic variables such as urban wind speed and humidity, which might affect the thermal environment. Second, the choice of study area and data timeliness could affect the universality of the conclusions. Future research could further combine data over a longer time scale for trend analysis and introduce more environmental factors and multi-variable models to comprehensively evaluate the overall impact of urban green spaces on the thermal environment. Additionally, how to achieve optimized green space layout and improve the sustainability of urban green space systems in the context of rapid urbanization will be an important direction for future research.

ACKNOWLEDGMENT

Research on the protection and inheritance strategy of Intangible Cultural Heritage in traditional villages of Henan Province based on cultural ecology, Henan Province Philosophy and Social Science Planning Project, 2023BYS035; Study on Intelligent Model Design for home care in the Age of Artificial Intelligence, Humanities and Social Science Project of Henan Education Department, 2025-ZDJH-783; Study on Cultural Spatial Reconstruction of Henan Woodcut New Year Pictures from the perspective of Spatial Production, Research Project of Intangible Cultural Heritage in Henan Province 2024-2025.

REFERENCES

[1] Bao, M., Zou, D.Z. (2024). The impact of architectural layout on urban heat island effect: A thermodynamic perspective. International Journal of Heat and Technology, 42(2): 520-528. https://doi.org/10.18280/ijht.420218

[2] Fardani, I., Putri, M. (2024). Spatio-Temporal analysis between landcover change and urban heat island. International Journal of Sustainable Development and Planning, 19(11): 4159-4166. https://doi.org/10.18280/ijsdp.191106

[3] Zhong, G.S., Wang, W.X. (2022). Optimization of the distribution of green buildings based on urban heat island effect. International Journal of Heat and Technology, 40(1): 333-338. https://doi.org/10.18280/ijht.400140

[4] Battista, G., Evangelisti, L., Guattari, C., De Cristo, E., De Lieto Vollaro, R., Asdrubali, F. (2023). An extensive study of the urban heat island phenomenon in Rome, Italy: Implications for building energy performance through data from multiple meteorological stations. International Journal of Sustainable Development and Planning, 18(11): 3357-3362. https://doi.org/10.18280/ijsdp.181101

[5] Gu, Y., Li, D. (2018). A modeling study of the sensitivity of urban heat islands to precipitation at climate scales. Urban Climate, 24: 982-993. https://doi.org/10.1016/j.uclim.2017.12.001

[6] Xu, T., Aini, A.M., Nordin, N.A. (2024). Utilizing regression model to characterize the impact of urban green space features on the subjective well-being of older adults. Heliyon, 10(15): e35567

[7] Yin, J., Fu, P., Cheshmehzangi, A., Li, Z., Dong, J. (2022). Investigating the changes in urban green-space patterns with urban land-use changes: A case study in Hangzhou, China. Remote Sensing, 14(21): 5410. https://doi.org/10.3390/rs14215410

[8] Feng, L., Wang, J., Liu, B., Hu, F., Hong, X., Wang, W. (2024). Does urban green space pattern affect green space noise reduction? Forests, 15(10): 1719.

[9] Meng, Q., Zhang, L., Wang, X., Hu, X., Allam, M., et al. (2024). Travel preference: An indicator of the benefits of urban green space. International Journal of Digital Earth, 17(1): 2342978. https://doi.org/10.1080/17538947.2024.2342978

[10] Wang, H., Feng, Y., Ai, L. (2023). Progress of carbon sequestration in urban green space based on bibliometric analysis. Frontiers in Environmental Science, 11: 1196803. https://doi.org/10.3389/fenvs.2023.1196803

[11] Li, Q., Thapa, S., Hu, X., Luo, Z., Gibson, D.J. (2022). The relationship between urban green space and urban expansion based on gravity methods. Sustainability, 14(9): 5396. https://doi.org/10.3390/su14095396

[12] Neema, M.N., Ohgai, A. (2013). Multitype green-space modeling for urban planning using GA and GIS. Environment and Planning B: Planning and Design, 40(3): 447-473. https://doi.org/10.1068/b38003

[13] Stessens, P., Khan, A.Z., Huysmans, M., Canters, F. (2017). Analysing urban green space accessibility and quality: A GIS-based model as spatial decision support for urban ecosystem services in Brussels. Ecosystem services, 28: 328-340. https://doi.org/10.1016/j.ecoser.2017.10.016

[14] Bertram, C., Rehdanz, K. (2015). The role of urban green space for human well-being. Ecological Economics, 120: 139-152. https://doi.org/10.1016/j.ecolecon.2015.10.013

[15] Stessens, P., Canters, F., Khan, A.Z. (2021). Exploring options for public green space development: Research by design and GIS-based scenario modelling. Sustainability, 13(15): 8213. https://doi.org/10.3390/su13158213

[16] Stessens, P., Canters, F., Huysmans, M., Khan, A.Z. (2020). Urban green space qualities: An integrated approach towards GIS-based assessment reflecting user perception. Land use policy, 91: 104319. https://doi.org/10.1016/j.landusepol.2019.104319

[17] Balram, S., Dragićević, S. (2005). Attitudes toward urban green spaces: Integrating questionnaire survey and collaborative GIS techniques to improve attitude measurements. Landscape and urban planning, 71(2-4): 147-162. https://doi.org/10.1016/j.landurbplan.2004.02.007

[18] Zhang, W. (2022). Design of urban garden landscape visualization system based on GIS and remote sensing

technology. Computational Intelligence and Neuroscience, 2022(1): 9592376. https://doi.org/10.1155/2022/9592376
[19] Dong, W. (2020). Research on energy saving planning of urban high-density green space based on digital remote sensing images. Fresenius Environmental Bulletin, 29(10): 9075-9081.
[20] Santos, T., Tenedório, J.A., Gonçalves, J.A. (2016). Quantifying the city's green area potential gain using remote sensing data. Sustainability, 8(12): 1247. https://doi.org/10.3390/su8121247
[21] Di Palma, M., Rigillo, M., Leone, M.F. (2024). Remote sensing technologies for mapping ecosystem services: An analytical approach for urban green infrastructure. Sustainability (2071-1050), 16(14): 1-24. https://doi.org/10.3390/su16146220
[22] Wang, J., Yin, P., Li, D., Zheng, G., Sun, B. (2021). Quantitative relationship between urban green canopy area and urban greening land area. Journal of Urban Planning and Development, 147(2): 05021016. https://doi.org/10.1061/(ASCE)UP.1943-5444.0000694
[23] Neyns, R., Canters, F. (2022). Mapping of urban vegetation with high-resolution remote sensing: A review. Remote Sensing, 14(4): 1031. https://doi.org/10.3390/rs14041031
[24] Xu, Z., Zhou, Y., Wang, S., Wang, L., Li, F., Wang, S., Wang, Z. (2020). A novel intelligent classification method for urban green space based on high-resolution remote sensing images. Remote Sensing, 12(22): 3845. https://doi.org/10.3390/rs12223845